A primer for manifestly gauge invariant computations in *SU*(*N*) Yang–Mills

2006 J. Phys. A: Math. Gen. 39 8699

(http://iopscience.iop.org/0305-4470/39/27/010)

INSTITUTE OF PHYSICS PUBLISHING JOURNAL OF PHYSICS A: MATHEMATICAL AND GENERAL

J. Phys. A: Math. Gen. **39** (2006) 8699–8726 doi:10.1088/0305-4470/39/27/010

A primer for manifestly gauge invariant computations in $SU(N)$ Yang–Mills

Oliver J Rosten

School of Physics and Astronomy, University of Southampton, Highfield, Southampton SO17 1BJ, UK

E-mail: O.J.Rosten@soton.ac.uk

Received 10 January 2006, in final form 5 May 2006
Published 21 June 2006
Online at stacks.iop.org/JPhysA/39/8699

Abstract

It has recently been determined that, within the framework of the exact renormalization group, continuum computations can be performed to any loop order in $SU(N)$ Yang–Mills theory without fixing the gauge or specifying the details of the regularization scheme. In this paper, we summarize and refine the powerful diagrammatic techniques which facilitate this procedure and illustrate their application in the context of a calculation of the two-loop β function.

PACS numbers: 11.10.Gh, 11.15.−q, 11.10.Hi

1. Introduction and conclusions

The exact renormalization group (ERG) has, for some time now, provided a framework allowing continuum computations in $SU(N)$ Yang–Mills theory to be performed without fixing the gauge [1–7]. Whilst being of obvious novelty value, manifest gauge invariance also provides several technical benefits. First, the gauge field is protected from field strength renormalization. Secondly, the Ward identities take a particularly simple form since the Wilsonian effective action is built only from gauge invariant combinations of the covariant derivative, even at the quantum level [1]. Thirdly, the difficult issue of Gribov copies [8]—which complicates non-perturbative studies in covariant gauges—is entirely avoided.

This latter point highlights the point that a manifestly gauge invariant formalism can, in many ways, be considered naturally adapted for non-perturbative problems. Indeed, the possibility of making statements about, e.g. confinement in an entirely gauge independent manner, is very appealing. It is perhaps, then, something of a stroke of luck that the manifestly gauge invariant scheme described in this paper is formulated within the framework of the ERG, since the ERG has a long and distinguished history as a powerful tool for studying non-perturbative phenomena [9–17].

The basic idea of the ERG—the continuum version of Wilson's renormalization group [18–20]—is that of integrating out degrees of freedom between the bare scale of a quantum

field theory and an effective scale, Λ. The effects of these modes are encoded in the Wilsonian effective action, S_Λ, which describes the physics of the theory in terms of parameters relevant to the effective scale. Central to the ERG methodology is the ERG (or flow) equation which determines how the Wilsonian effective action changes under infinitesimal changes of the scale. It is by relating physics at different scales, in this way, that the ERG provides access to non-perturbative phenomena.

There have been several different attempts to adapt the ERG for non-Abelian gauge theory (for a comprehensive review, see [21]). However, all of these must face up to the problem that, at least naïvely, the implementation of a momentum cutoff (which is fundamental to the ERG) breaks non-Abelian gauge invariance. The traditional solution to this problem is to accept this breaking, recovering the physical symmetry in the limit that all quantum fluctuations have been integrated out [22–29]. In contrast, the scheme employed in this paper utilizes a regularization scheme based on a real, gauge invariant cutoff, Λ [30]. In this way (manifest) gauge invariance is maintained at all scales.

Though the earliest formulation of a manifestly gauge invariant ERG [1, 2] was constructed in the large N-limit, its subsequent refinement [3] facilitated the first manifestly gauge invariant calculation of the one-loop β function, β_1, at finite N. Guided by the universality of the answer, the calculation of β_1 was performed without specifying the precise details of the regularization scheme, leading to a partially diagrammatic computational methodology.

However, preserving these diagrammatic techniques beyond one loop required generalization of the flow equation. The reason for this is as follows. The implementation of the gauge invariant cutoff is achieved by embedding the physical $SU(N)$ theory in a spontaneously broken $SU(N|N)$ supergauge theory [30]. Besides the coupling, $g(\Lambda)$, of the physical $SU(N)$ gauge field, A^1_μ, there is a second coupling, $g_2(\Lambda)$, associated with an unphysical $SU(N)$ field, A^2_μ, that requires separate renormalization [4–6][1]. As a direct consequence of this, the diagrammatic tricks can only be maintained if the flow equation treats A^1 and A^2 independently, in the broken phase. This challenging problem, finally overcome in [5, 6], yielded the first manifestly gauge invariant, continuum calculation of the two-loop β function [5, 7], β_2. The practical execution of this calculation necessitated the major development of the original diagrammatic techniques, not only for calculational convenience, but also to elucidate the structure of the new or flow equation [5–7].

The considerable amount of detail present in [5–7] reflects the subtlety and complexity of the new flow equation. However, the actual rules for performing perturbative calculations are remarkably simple, as a consequence of the diagrammatics. In this paper, we summarize the primary diagrammatic rules and use the illustration of their application to significantly refine the calculational procedure of [6] (see also [5]). Though performing an actual β-function calculation is still more complicated than in alternative approaches, the developments of this paper allow a further radical simplification which we will discuss later.

Contrary to previous works [3–6], the flow equation is introduced via its diagrammatic representation. Hence, we do not work with a single flow equation but rather with an infinite class which obey the same diagrammatic rules. (It is assumed that the general properties which all good flow equations possess [3, 4, 31–33], e.g. invariance of physics under the flow, are implicitly satisfied.)

Within our ERG, the flow is controlled by a (generically) non-universal object, $\hat{S}$, the 'seed action' [3, 5–7, 32–34]. This respects the same symmetries as the Wilsonian effective action, S, and has the same structure. However, whereas our aim is to solve the flow for S, $\hat{S}$

[1] For technical reasons, a superscalar field is given zero mass dimension [3], and thus is associated by the usual dimensional reasoning with an infinite number of dimensionless couplings. These couplings do not require renormalization [5, 7].

acts as an input. In accord with our general philosophy, the seed action is left unspecified where possible and implicitly defined where necessary. There is one important exception to this, at the heart of the diagrammatic techniques: it is technically useful to set the two-point, tree level seed action vertices equal to their Wilsonian effective action counterparts. In turn, this ensures that, if the flow equation is sufficiently general [6], then for each independent two-point, tree level vertex (that cannot be consistently set to zero) there exists an 'effective propagator', which plays a crucial diagrammatic role. These effective propagators, denoted by Δ, are the inverses of the two-point, tree level vertices up to remainder terms [3] (in the gauge sector); we call this the 'effective propagator relation' [3]. The remainder terms appear as a consequence of the manifest gauge invariance: the effective propagators are inverses of the two-point, tree level vertices only in the transverse space. It is important to emphasize that the effective propagators are by no means propagators in the usual sense, but their name recognizes their similarity in both form and diagrammatic function.

In this paper, we will indicate in some detail how, starting from a diagrammatic expression for β_2 involving the seed action and details of the covariantization of the cutoff, we can derive an expression with no explicit dependence on these non-universal objects. The basic strategy is to recognize that amongst the terms generated by the flow equation are manipulable diagrams comprising exclusively Wilsonian effective action vertices joined together by a differentiated effective propagator. These latter objects are denoted by $\dot{\Delta}$ where, having defined

$$\alpha \equiv \frac{g_2^2}{g^2}, \tag{1}$$

we define

$$\dot{X} \equiv -\Lambda\partial_\Lambda|_\alpha X, \tag{2}$$

$\Lambda\partial_\Lambda$ being the generator of the ERG flow. The manipulable diagrams are processed by moving $\Lambda\partial_\Lambda|_\alpha$ from the effective propagator to strike the diagram as a whole, minus correction terms in which $\Lambda\partial_\Lambda|_\alpha$ strikes the vertices. The former terms, called Λ-derivative terms, are those from which the numerical value of β_2 can be directly extracted [5, 7]; the latter terms can be processed using the flow equation and the resulting set of diagrams simplified, using primary diagrammatic identities. At this point, we are able to identify cancellations of non-universal contributions, at the diagrammatic level. There is, however, a complication to this diagrammatic procedure: particular classes of sub-diagrams can have two distinct diagrammatic representations. The equivalence of these representations is encoded in the secondary diagrammatic identities, of which a sub-set is presented here. (For the complete set, the reader is referred to [36].)

Iterating the above procedure, the diagrammatic expression can be reduced exclusively to Λ-derivative terms and 'α-terms'. These latter terms explicitly involve the flow of α and are an artefact of the $SU(N|N)$ regularization scheme. Subject to very general constraints, they vanish, as they must, in the limit that $\alpha \to 0$ [5, 7].

Compared with [6], we realize that, at each stage of the calculation, both the cancellation of sets of non-universal contributions and the creation of sets of Λ-derivative terms can each be done in parallel. This vastly simplifies the calculational procedure, the benefits becoming increasingly pronounced with each loop order. Despite this important development, even at two-loops a β function calculation still has many steps. However, the illustration of the β_2 diagrammatics will serve to demonstrate that the procedure is algorithmic. As we will see in [35, 36] (see also [5] for an incomplete discussion), this can be turned very much to our advantage: using the techniques of this paper, we can jump straight from the initial expression for a β function coefficient to the Λ-derivative and α-terms, *to all orders in perturbation theory*.

At a stroke, this removes the major difficulty associated with performing computations within our framework, leaving open the exciting prospect of a manageable, manifestly gauge invariant calculus for $SU(N)$ Yang–Mills theory.

Section 2 introduces the necessary elements of $SU(N|N)$ gauge theory, for our purposes. In section 3 we describe the diagrammatics. First, we give the diagrammatic representation of the exact flow equation. Secondly, we describe the diagrammatic realization of the Ward identities. Thirdly, we show how the various vertices of the objects involved in the flow equation can be Taylor expanded. Lastly, we specialize the diagrammatics to the perturbative domain. In section 5, we illustrate the use of the diagrammatics in the context of a computation of the perturbative two-loop β function.

2. Elements of $SU(N|N)$ gauge theory

Throughout this paper, we work in Euclidean dimension, D. We regularize $SU(N)$ Yang–Mills by embedding it in spontaneously broken $SU(N|N)$ Yang–Mills, which is itself regularized by covariant higher derivatives [30]. The supergauge field, $\mathcal{A}_\mu$, is valued in the Lie superalgebra and, using the defining representation, can be written as a Hermitian supertraceless supermatrix:

$$\mathcal{A}_\mu = \begin{pmatrix} A^1_\mu & B_\mu \\ \bar{B}_\mu & A^2_\mu \end{pmatrix} + \mathcal{A}^0_\mu \mathbb{1}.$$

Here, $A^1_\mu(x) \equiv A^1_{a\mu}\tau^a_1$ is the physical $SU(N)$ gauge field, τ^a_1 being the $SU(N)$ generators orthonormalized to $\mathrm{tr}\left(\tau^a_1\tau^b_1\right) = \delta^{ab}/2$, while $A^2_\mu(x) \equiv A^2_{a\mu}\tau^a_2$ is a second unphysical $SU(N)$ gauge field. The B fields are fermionic gauge fields which will gain a mass of order Λ from the spontaneous symmetry breaking; they play the role of gauge invariant Pauli–Villars (PV) fields, furnishing the necessary extra regularization to supplement the covariant higher derivatives.

The theory is locally invariant under

$$\delta\mathcal{A}_\mu = [\nabla_\mu, \Omega(x)] + \lambda_\mu \mathbb{1}. \tag{3}$$

The first term, in which $\nabla_\mu = \partial_\mu - \mathrm{i}\mathcal{A}_\mu$, generates supergauge transformations. Note that the coupling, g, has been scaled out of this definition. It is worth doing this: since we do not gauge fix, the exact preservation of (3) means that none of the fields suffer field strength renormalization, even in the broken phase [3].

The second term in (3) divides out the centre of the algebra. This 'no $\mathcal{A}^0$ shift symmetry' ensures that nothing depends on $\mathcal{A}^0_\mu$ and that $\mathcal{A}^0_\mu$ has no degrees of freedom. We adopt a prescription whereby we can effectively ignore the field $\mathcal{A}^0_\mu$, altogether, using it to map us into a particular diagrammatic picture [5, 6].

For the superscalar field, $\mathcal{C}$, which spontaneously breaks the $SU(N|N)$ invariance, there is no need to factor out the central term [30] and so we write

$$\mathcal{C} = \begin{pmatrix} C^1 & D \\ \bar{D} & C^2 \end{pmatrix}.$$

This field transforms covariantly:

$$\delta\mathcal{C} = -\mathrm{i}[\mathcal{C}, \Omega].$$

In order that, at the classical level, the spontaneous breaking scale tracks the covariant higher derivative effective cutoff scale, Λ, we take $\mathcal{C}$ to be dimensionless and demand that $\hat{S}$ has the minimum of its effective potential at

$$\langle\mathcal{C}\rangle = \sigma \equiv \begin{pmatrix} \mathbb{1} & 0 \\ 0 & -\mathbb{1} \end{pmatrix}. \tag{4}$$

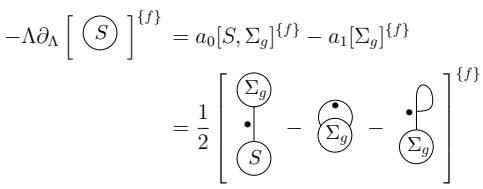

Figure 1. The diagrammatic form of the flow equation.

In this case the classical action S_0 also has a minimum at (4). Ensuring that this is not destroyed by quantum corrections demands that the Wilsonian effective action one-point C^1, C^2 vertices vanish [3, 5, 6], which can be translated into a constraint on $\hat{S}$.

Working in the broken phase, the fermionic fields B_μ, $\bar{B}_\nu$ and D, $\bar{D}$ can be combined into the fields,

$$F_M = (B_\mu, D), \tag{5a}$$
$$\bar{F}_N = (\bar{B}_\nu, -\bar{D}), \tag{5b}$$

where M, N are five-indices [5–7][2]. This simplification recognizes that, via the Higgs mechanism, B and D gauge transform into each other and so propagate together.

In $SU(N|N)$ gauge theory, the supertrace replaces the trace as the natural cyclic invariant [30, 37]. The manifestly gauge invariant Wilsonian effective action, S, comprises supertraces and products of supertraces where the arguments of the supertraces are sets of net-bosonic fields.

3. Diagrammatics

In recognition of the central role played by the diagrammatics, our approach is generally to first state the diagrammatic rules and then to describe the various elements involved.

3.1. The exact flow equation

The ERG equation can be represented as shown in figure 1 [5, 6].

The left-hand depicts the flow of all independent Wilsonian effective action vertex *coefficient functions*, which correspond to the set of fields, $\{f\}$. Each coefficient function has associated with it an implied supertrace structure (and symmetry factor which, as one would want, does not appear in the diagrammatics). For example,

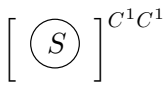

(6)

represents both the coefficient functions $S^{C^1C^1}$ and S^{C^1,C^1} which, respectively, are associated with the supertrace structures $\mathrm{str}\, C^1C^1$ and $\mathrm{str}\, C^1 \mathrm{str}\, C^1$.

The first diagram on the right-hand side of figure 1 is a formed by the bilinear functional $a_0[S, \Sigma_g]$, whereas the next two diagrams are formed by $a_1[\Sigma_g]$. All three diagrams have two different components. The lobes represent vertices of action functionals, where

[2] The summation convention for these indices is that we take each product of components to contribute with unit weight.

$\Sigma_g \equiv g^2 S - 2\hat{S}$. The object attaching to the various lobes, —•—, is the sum over vertices of the covariantized ERG kernels [1, 3] and, like the action vertices, can be decorated by fields belonging to $\{f\}$. The fields of the action vertex (vertices) to which the vertices of the kernels attach act as labels for the ERG kernels though, in certain circumstances, the particular decorations of the kernel are required for unambiguous identification [5, 6]. However, in actual calculations, these non-universal details are irrelevant. We loosely refer to both individual and summed over vertices of the kernels simply as a kernel. Note that kernels labelled at one end by either A or B and at the other by either C or D do not exist [3].

The final diagram on the right-hand side contains a kernel which 'bites its own tail'. Such diagrams are not properly UV regularized by the $SU(N|N)$ regularization and, in the past, it has been argued that they can be discarded [1, 3, 6, 38][3]. Here, though, we will keep these diagrams: as recognized in [5], in any calculation of universal quantities, all explicit instances of diagrams in which a kernel bites its tail (which can always be dimensionally regularized) are cancelled by implicit instances buried in other terms. We will see an example of this in section 5.

At this point, it is worth drawing attention to a subtlety of the $SU(N|N)$ regularization scheme. For the scheme to be properly defined, a preregularizer must be used [30]. For convenience, this has traditionally been taken to be dimensional regularization. However, this amounts to a choice which is by no means unique. Indeed, as we shall see, there are strong hints that there is an entirely diagrammatic prescription that can be used instead, which would make sense in $D = 4$. Thus, using dimensional regularization to regularize diagrams in which the kernels bite their own tails is distinct from its previous application as just a preregularizer.

The rule for decorating the complete diagrams on the right-hand side is simple: the set of fields, $\{f\}$, are distributed in all independent ways between the component objects of each diagram.

Embedded within the diagrammatic rules is a prescription for evaluating the group theory factors. Suppose that we wish to focus on the flow of a particular vertex coefficient function, which necessarily has a unique supertrace structure. For example, we might be interested in just the $S^{C^1 C^1}$ component of (6).

On the right-hand side of the flow equation, we must focus on the components of each diagram with precisely the same supertrace structure as the left-hand side, noting that the kernel, like the vertices, has multi-supertrace contributions (for more details see [5, 6]). In this more explicit diagrammatic picture, the kernel is to be considered a double-sided object. Thus, whilst the dumbbell like term of figure 1 has at least one associated supertrace, the next two diagrams has at least two, on a account of the loop (this is strictly true only in the case that kernel attaches to fields on the same supertrace). If a closed circuit formed by a kernel is devoid of fields then it contributes a factor of $\pm N$, depending on the flavours of the fields to which the kernel forming the loop attaches. This is most easily appreciated by defining the projectors

$$\sigma_+ \equiv \begin{pmatrix} \mathbb{1} & 0 \\ 0 & 0 \end{pmatrix}, \qquad \sigma_- \equiv \begin{pmatrix} 0 & 0 \\ 0 & \mathbb{1} \end{pmatrix}$$

and noting that $\operatorname{str} \sigma_\pm = \pm N$. In the counterclockwise sense, a σ_+ can always be inserted after an A^1, C^1 or $\bar{F}$, whereas a σ_- can always be inserted after an A^2, C^2 or F.

[3] These diagrams are artefacts of the flow equation. The $SU(N)$ gauge theory *is* fully regularized by the $SU(N|N)$ scheme. However, regularization of the flow equation does not trivially follow from the regularization of the underlying theory.

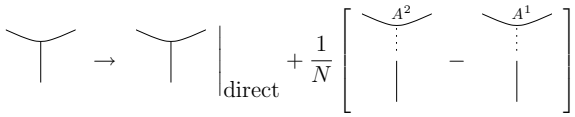

Figure 2. The $1/N$ corrections to the group theory factors.

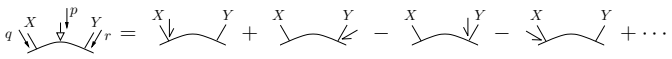

Figure 3. The Ward identities.

The rules thus described receive $1/N$ corrections in the A^1 and A^2 sectors. If a kernel attaches to an A^1 or A^2, it comprises a direct attachment and an indirect attachment, as shown in figure 2 (see [5, 6] for more detail).

We can thus consider the diagram on the left-hand side as having been unpackaged, to give the terms on the right-hand side. The dotted lines in the diagrams with indirect attachments serve to remind us where the loose end of the kernel attaches in the parent diagram.

3.2. Ward identities

3.2.1. Application to isolated vertices. All vertices, whether they belong to either of the actions or to the covariantized kernels, are subject to Ward identities. Due to the manifest gauge invariance, these take a particularly simple form, as shown in figure 3. This is our first example of a primary diagrammatic identity.

On the left-hand side, we contract a vertex with the momentum of the field which carries p. This field—which we will call the active field—can be either A^1_ρ, A^2_ρ, F_R or $\bar{F}_R$. In the first two cases, the open triangle $\triangleright$ represents p_ρ whereas, in the latter two cases, it represents $p_R \equiv (p_\rho, 2)$ [5, 6]. (Given that we often sum over all possible fields, we can take the Feynman rule for $\triangleright$ in the C-sector to be null.) In all cases, $\triangleright$ is independent of Λ and α, which is encoded in the following primary diagrammatic identities:

$$\overset{\bullet}{\triangleright} \quad = 0, \tag{7a}$$

$$\overset{\text{@}}{\triangleright} \quad = 0, \tag{7b}$$

where $\text{@} \equiv \partial/\partial\alpha$.

On the right-hand side, we push the contracted momentum forward onto the field which directly follows the active field, in the counterclockwise sense, and pull back (with a minus sign) onto the field which directly precedes the active field. Since our diagrammatics is permutation symmetric, the struck field—which we will call the target field—can be either X, Y or any of the undrawn fields represented by the ellipsis. Any field(s) besides the active field and the target field will be called spectators. Note that we can take X and/or Y to represent the end of a kernel. In this case, the struck field is determined to be unambiguously on one side of the (double sided) kernel; the contributions in which the struck field is on the other side are included in the ellipsis. This highlights the point that allowing the active field to strike another field necessarily involves a partial specification of the supertrace structure: it must be

the case that the struck field either directly followed or preceded the active field. In turn, this means that the Feynman rule for particular choices of the active and target fields can be zero. For example, an F can follow, but never precede an A^1_μ, and so the pull back of an A^1_μ onto an F should be assigned a value of zero. The momentum routing follows in obvious manner: for example, in the first diagram on the right-hand side, momentum $q + p$ now flows into the vertex. In the case that the active field is fermionic, the field pushed forward/pulled back onto is transformed into its opposite statistic partner. There are some signs associated with this in the C- and D-sectors, which we will not require here [5, 6]; for calculations of universal quantities, they are hidden by the diagrammatics.

The half arrow which terminates the pushed forward/pulled back active field is of no significance and can go on either side of the active field line. It is necessary to keep the active field line—even though the active field is no longer part of the vertex—in order that we can unambiguously deduce flavour changes and momentum routing, without reference to the parent diagram.

We illustrate the application of the Ward identities by considering contracting $\triangleright$ into the Wilsonian the effective action two-point vertex:

(8)

Given that $\triangleright$ is null in the C^i sector, the fields decorating the two-point vertex on the right-hand side can be either both A^is or both fermionic. In the former case, (8) reads

$$p_\mu S^{A^i\,A^i}_{\mu\ \ \nu}(p) = S^{A^i}_\nu(0) - S^{A^i}_\nu(0) = 0,$$

where we note that $S^{A^i}_\nu$ is in fact zero by itself, as follows by both Lorentz invariance and gauge invariance. In the latter case, (8) reads

$$p_M S^{\bar{F}F}_{MN}(p) = S^{C^2}(0) - S^{C^1}(0),$$

where we have used (5*a*) and have discarded contributions which go like $S^{A^i}_\nu(0)$. However, the $S^{C^i}(0)$ must vanish. This follows from demanding that the minimum of the superhiggs potential is not shifted by quantum corrections [3]. Therefore, we arrive at the diagrammatic identity

(9)

3.2.2. Application to complete diagrams. Consider the flow of a (Wilsonian effective action) vertex which is contracted with the momentum of one of its fields. Suppose that, in a addition to the active field, the vertex is decorated by the set of fields $\{f'\}$. Referring back to figure 1, the left-hand side becomes the sum of vertices decorated by $\{f'\}$ where, for each diagram in the sum, one of the elements of $\{f'\}$ is either pushed forward or pulled back onto by the active field.

The right-hand side of figure 1 now comprises three different types of diagram. The active field can either push forward or pull back

(i) onto one of the elements of $\{f'\}$;
(ii) round an action vertex onto an internal field;
(iii) onto the end of a kernel.

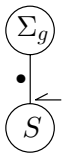

Figure 4. Example of a diagram in which the active field strikes an internal field.

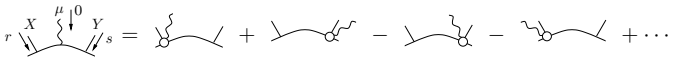

Figure 5. Diagrammatic representation of zeroth-order Taylor expansion.

An example of a diagrams of either the second or third type is shown in figure 4.

Recalling that, if the active field is fermionic, the flavour of the struck field will change, attachment corrections of the type shown in figure 2 must be worked out *after* the action of the active field, and according to whether the field attached *to* (rather than the field at the end of the kernel, which will be of a different flavour) is in the $A^{1,2}$ sector [5].

By gauge invariance, it must be the case that the sum over all diagrams of the second and third types vanishes [6] (see [5] for an explicit demonstration of this). This follows since we are simply computing the flow of a vertex (albeit one in which one of the fields can be though of as having been struck by a active field). From figure 1, we know that there cannot be any surviving contributions in which internal fields are pushed forward/pulled back onto[4].

3.3. Taylor expansion of vertices

For the formalism to be properly defined, it must be the case that all vertices are Taylor expandable to all orders in momenta [1, 2, 10]. For the purposes of this paper, we need only the diagrammatic rules for a particular scenario. Consider a vertex which is part of a complete diagram, decorated by some set of internal fields and by a single external A^1 (or A^2). The diagrammatic representation for the zeroth-order expansion in the momentum of the external field is all that is required and is shown in figure 5 [5, 6]; note the similarity to figure 3.

The interpretation of the diagrammatics is as follows. In the first diagram on the right-hand side, the vertex is differentiated with respect to the momentum carried by the field X, whilst holding the momentum of the preceding field fixed (if the preceding field carries zero momentum, it is effectively transparent to the momentum derivative [6] and so we go in a clockwise sense to the first field which carries non-zero momentum to determine the momentum held constant). Of course, using our current diagrammatic notation, this latter field can be any of those which decorate the vertex, and so we sum over all possibilities. Thus, each cyclically ordered push forward like term has a partner, cyclically ordered pull back like term, such that the pair can be interpreted as

$$\left(\partial_\mu^r\big|_s - \partial_\mu^s\big|_r\right)\text{Vertex}, \tag{10}$$

where r and s are momenta entering the vertex. In the case that $r = -s$, we can and will drop either the push forward like term or pull back like term, since the combination can be expressed as ∂_μ^r; we interpret the diagrammatic notation appropriately. Just as in figure 3, the fields X and

[4] In β function calculations, where active fields arise in a different context, diagrams in which internal fields are pushed forward/pulled back onto can survive.

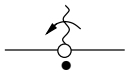

Figure 6. Notation for the derivative with respect to the momentum entering an undecorated kernel.

or Y can be interpreted as the end of a kernel. In this case, we introduce some new notation, since it proves confusing in complete diagrams to actually locate the derivative symbol at the end of such an object. The notation for the derivative with respect to the momentum entering the end of a kernel is introduced in figure 6.

Recalling that a kernel, whose fields are explicitly cyclically ordered, is a two-sided object, we first note that the field whose momentum we have expanded in is sat on the topside of the vertex. The derivative is taken to be with respect to the momentum which flows *into* the end of the vertex which follows the derivative, in the sense indicated by the arrow on the derivative symbol. It is clear that the direction of the arrow on the derivative symbol can be reversed at the expense of a minus sign.

3.4. Charge conjugation invariance

Charge conjugation invariance can be used to simplify the diagrammatics, by allowing us to discard certain terms and to combine others. The diagrammatic rule for replacing a diagram with its charge conjugate is to reflect the diagram, picking up a sign for every external A^1 or A^2 and letting $\bar{F} \leftrightarrow F$ [5, 6] (we temporarily assume that no Taylor expansions have been performed and that, should any of the fields be contracted with their momentum, the Ward identities are yet to be applied).

Charge conjugation is of particular use in complete diagrams for which all external fields are bosonic. In this case, charge conjugation effectively never changes field flavours. The only such changes induced by charge conjugation are in the fermionic sector where, after reflection, we must change $\bar{F} \leftrightarrow F$. However, by taking all external fields to be bosonic, these changes now only affect internal fields, whose flavours are summed over anyway.

Thus, for example, a diagram possessing only bosonic external fields (and any number of internal fields) must possess an even number of external $A^{1,2}$ fields but any number of external $C^{1,2}$ fields.

It is straightforward to extend the diagrammatic rule for charge conjugation to include diagrams containing momentum derivatives and/or application of the Ward identities [5, 6]. Supplementing the previous rule, we simply pick up a minus sign for each momentum derivative and for each application of the Ward identities [5, 6]. Note that active fields which have been processed by the Ward identities should still be counted when we sum up the number of external A^1s and A^2s; this is intuitive from a diagrammatic point of view, since the field line is kept, but now terminates in a half arrow, rather then entering a vertex.

This allows us to simplify the set of terms generated either by an application of the Ward identities or by a Taylor expansion. To illustrate this, we need deal only the former case, due to the similarity of the diagrammatic rules for each. Consider a diagram generated by a single application of the Ward identities, in which no Taylor expansions have been performed. We focus on a single target field, which we know can be both pushed forward and pulled back onto, as shown in figure 7.

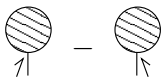

Figure 7. Sum of the push forward and pull back onto the same target field.

The assumption that the diagram contains no further target fields or momentum derivatives tells us that the supertrace structure of all spectator fields is unspecified. That all external fields are bosonic ensures that charge conjugation leaves the field content of the diagram unchanged. Thus, reflecting either diagram of figure 7, we can combine terms with the other diagram. Whether contributions add or cancel depends on whether the diagrams as a whole are charge conjugation odd or even.

Given that we have combined terms in this way, suppose that there is a second active field (or that we perform a Taylor expansion). Using the Ward identities, we once again find that each target field is both pushed forward and pulled back onto. Now, however, such terms cannot be combined, since the supertrace structure of the fields which spectate with respect to this second application of the Ward identities has a partially specified supertrace structure, themselves. Consider the complete set of diagrams generated by any number of applications of the Ward identities and possessing any number of momentum derivatives. For each factorizable sub-diagram, we can combine one push forward with one pull back; thereafter, we cannot combine terms further.

In our example calculation of β_2, we will encounter active fields attached to internal lines. Since the flavour of internal lines is summed over, we can combine pushes forward with pulls back of these fields, using the recipe above.

3.5. Perturbative diagrammatics

In the perturbative domain, we have the following weak coupling expansions [1, 3, 5, 6]. The Wilsonian effective action is given by

$$S = \sum_{i=0}^{\infty} (g^2)^{i-1} S_i = \frac{1}{g^2} S_0 + S_1 + \cdots, \tag{11}$$

where S_0 is the classical effective action and the $S_{i>0}$ the ith loop corrections. The seed action has a similar expansion:

$$\hat{S} = \sum_{i=0}^{\infty} g^{2i} \hat{S}_i. \tag{12}$$

Recalling (1) we have

$$\beta \equiv \Lambda \partial_\Lambda g = \sum_{i=1}^{\infty} g^{2i+1} \beta_i(\alpha) \tag{13}$$

$$\gamma \equiv \Lambda \partial_\Lambda \alpha = \sum_{i=1}^{\infty} g^{2i} \gamma_i(\alpha). \tag{14}$$

3.5.1. The weak coupling flow equations. Defining $\Sigma_i = S_i - 2\hat{S}_i$, the weak coupling flow equations follow from substituting (11)–(14) into the flow equation, as shown in equation (15) [5, 6].

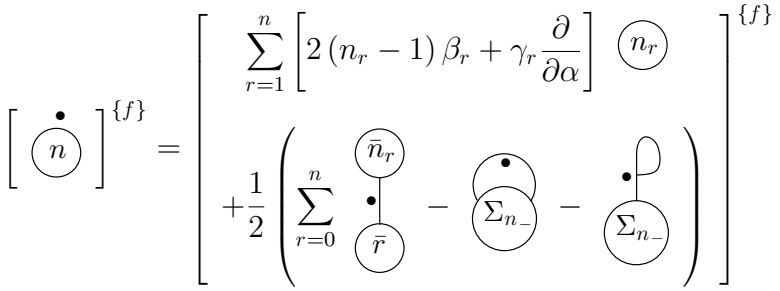

(15)

We refer to the first two terms on the right-hand side of (15) as β- and α-terms, respectively. The symbol $\bullet$, as in equation (2), means $-\Lambda\partial_\Lambda|_\alpha$. A vertex whose argument is an unadorned letter, say n, represents S_n. We define $n_r \equiv n - r$ and $n_\pm \equiv n \pm 1$. The bar notation of the dumbbell term is defined as follows:

$$a_0[\bar{S}_{n-r}, \bar{S}_r] \equiv a_0[S_{n-r}, S_r] - a_0[S_{n-r}, \hat{S}_r] - a_0[\hat{S}_{n-r}, S_r].$$

3.5.2. The effective propagator relation. The effective propagator relation [3] is central to the perturbative diagrammatic approach, and arises from examining the flow of all two-point, tree level vertices. This is done by setting $n = 0$ in (15) and specializing $\{f\}$ to contain two fields, as shown in equation (16). We note that we can and do choose all such vertices to be single supertrace terms [5, 6].

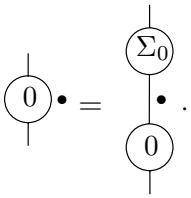

(16)

Following [1–3, 5, 6, 33, 38], we use the freedom inherent in $\hat{S}$ by choosing the two-point, tree level seed action vertices equal to the corresponding Wilsonian effective action vertices. Equation (16) now simplifies. Rearranging, integrating with respect to Λ and choosing the appropriate integration constants [5, 6], we arrive at the relationship between the integrated ERG kernels—also known as the effective propagators—and the two-point, tree level vertices shown in equation (17). Note that we have attached the effective propagator, which only ever appears as an internal line, to an arbitrary structure (this attachment ensures that the prescription for evaluating the group theory factors, and not just the algebra, matches between the two sides of the equation).

(17)

We have encountered $\triangleright$ already, in section 3.2. Of $>$, all we need know for our purposes is that it carries an index, M, which is a four-index in the A^1, A^2 sectors, and a five index in the F, $\bar{F}$ sectors. In the C sector, $>$ is null [3, 5, 6]. The structure $>\triangleright$ is a 'gauge remainder' [3]. The individual components of $>\triangleright$ will often be loosely referred to as gauge remainders; where

it is necessary to unambiguously refer to the composite structure, we will use the terminology 'full gauge remainder'.

It is important to note that we have defined the diagrammatics in equation (17) such that there are no $1/N$ corrections where the effective propagator attaches to the two-point, tree level vertex. We do this because, when the composite object on the left-hand side of equation (17) appears in actual calculations, it always occurs inside some larger diagram. It is straightforward to show that, in this case, the aforementioned attachment corrections always vanish [5].

3.5.3. Further diagrammatic identities. The following diagrammatic identities all follow from the ones stated already. However, since they are so heavily used in perturbative calculations we give them in their own right, particularly as not all of them are immediately obvious.

The first of these, though, is trivial, following directly from (9):

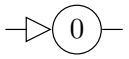

$$= 0. \tag{18}$$

From the effective propagator relation and (18), two further diagrammatic identities follow. First, consider attaching an effective propagator to the right-hand field in (18) and applying the effective propagator before $\triangleright$ has acted. Diagrammatically, this gives

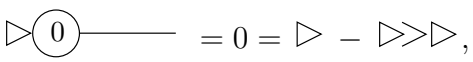

which implies the following diagrammatic identity:

$$= 1. \tag{19}$$

The effective propagator relation, together with (19), implies that

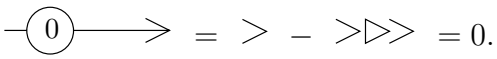

In other words, the (non-zero) structure $\rightarrow$ kills a two-point, tree level vertex. But, by (18), this suggests that the structure $\rightarrow$ must be equal, up to some factor, to $\triangleleft$. Indeed,

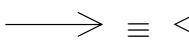

$$\equiv \tag{20}$$

where the dot–dash line represents the pseudo-effective propagators of [5, 6].

4. Universality

To compute a universal quantity, we must feed in a physical input, which is done via the renormalization condition [1, 3]:

$$S[\mathcal{A} = A^1, \mathcal{C} = \bar{\mathcal{C}}] = \frac{1}{2g^2}\,\mathrm{tr}\int \mathrm{d}^D x\ \left(F^1_{\mu\nu}\right)^2 + \cdots, \tag{21}$$

where the ellipsis denotes higher dimension operators and ignored vacuum energy and $\bar{\mathcal{C}}$ is the location of the minimum of the Higgs potential. This forces

$$S^{11}_{0\mu\nu}(p) = 2\,\Box_{\mu\nu}(p) + \mathcal{O}(p^4),$$

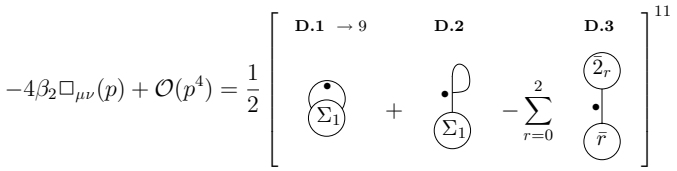

Figure 8. Diagrammatic equation for β_2.

where the 1s are shorthand for A^1s and the $\mathcal{O}(p^4)$ contributions to the vertex are non-universal. We can arrange calculations of universal β function coefficients and, presumably, of all universal quantities such that the answer is manifestly controlled by the renormalization condition [5–7, 34].

When computing β_2, we must remove all contributions arising from the running of α in order to obtain agreement with the standard, universal answer; this is done by tuning $\alpha \to 0$ at the end of the calculation [5–7].[5] Note that the γ_i of (14) are determined by the renormalization condition for the unphysical coupling, g_2:

$$S[\mathcal{A}=A^2,\mathcal{C}=\bar{\mathcal{C}}]=-\frac{1}{2\alpha g^2}\,\mathrm{tr}\int \mathrm{d}^D x\,\left(F^2_{\mu\nu}\right)^2+\cdots.$$

5. Illustration

To illustrate the diagrammatic techniques in action, we will perform the initial stages of a computation of β_2. To start, we specialize the weak coupling flow equations (15) to $n=2$, take $\{f\}=A^1_\mu A^1_\nu$ and work at $\mathcal{O}(p^2)$. The renormalization condition (21) implies that $S^{11}_{\geqslant 1\mu\nu}(p)\sim\mathcal{O}(p^4)$ and so we are left with an algebraic equation for β_2, as shown in figure 8. The Lorentz indices of the external fields are suppressed.

Diagrams are labelled in boldface. If a diagram is cancelled, then its reference number is enclosed in curly braces, together with the reference number of the diagram against which it cancels. If the reference number of a diagram is followed by an arrow, the arrow points to the figure where the diagram is processed. Since we are not performing the complete diagrammatics for β_2, not all diagrams are labelled and, of those that are, not all are processed or cancelled.

When explicitly decorating with the external fields, we note that they are identical, by Bose symmetry. Thus, for terms in which the two fields decorate separate structures, we can simply draw a single diagram but pick up a factor of 2.

For each diagram generated by the flow, our strategy is as follows. First, we isolate the component for which all vertices are Wilsonian effective action vertices and for which the kernel is undecorated, should it exist. To facilitate this separation, we introduce the symbol $\odot$ to indicate an undecorated kernel and $\circ$ such that, when operating on a kernel, $\bullet=\odot+\circ$. In certain circumstance, we will be able to trade symbols; for example, if a kernel carries $\circ$ but possesses an explicit decoration, then we can replace $\circ$ by $\bullet$. The manipulable component of diagram D.1 is isolated in figure 9.

[5] Of course, disagreement with the standard value of β_2 is not necessarily a signature of a sick formalism, since β_2 is not physically observable and is only expected to agree between two differing schemes under certain conditions.

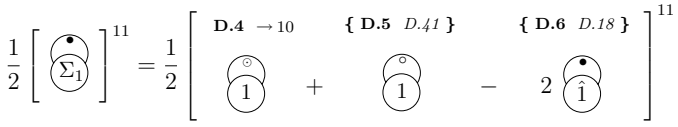

Figure 9. Isolating the manipulable component for diagram D.1.

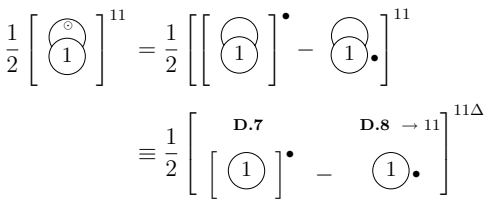

Figure 10. Converting diagram D.4 into a Λ-derivative term.

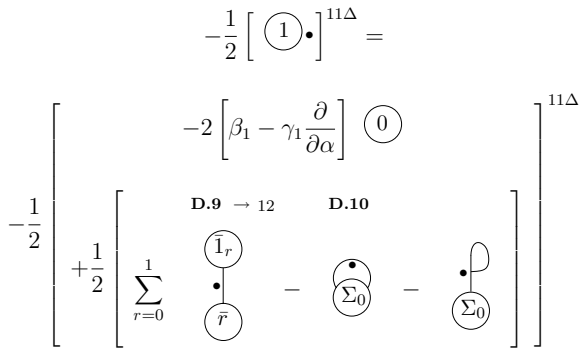

Figure 11. Result of processing diagram D.8 with the one-loop flow equation.

Notice that this diagrammatic step has been performed without explicitly decorating terms with the external fields, thereby reducing the number of terms we have to deal with. This is the first refinement of the computational methodology employed in [6].

Next, there follows a two-step process. First, we convert diagram D.4 into a Λ-derivative term, by moving the Λ-derivative off the effective propagator. This is shown in the first line of figure 10. On the second line, we promote the effective propagator to an implicit decoration; this promotion is the second refinement of the diagrammatics.

Notice that we have replaced $\odot$ by $\bullet$, since we take these symbols to mean the same thing, i.e. just $-\Lambda\partial_\Lambda|_\alpha$, when operating on a vertex or effective propagator.

Diagram D.7 is a Λ-derivative term. The vertex is enclosed in square brackets which tells us that $-\Lambda\partial_\Lambda|_\alpha$ is taken to act *after explicit decoration*. However, in diagram D.8, it is just the vertex which is struck by $-\Lambda\partial_\Lambda|_\alpha$; this term is processed using the flow equation, as shown in figure 11.

There now follows a crucial step in the diagrammatic procedure: we recognize that diagram D.9 possesses two-point, tree level vertices that can be attached to either the external fields or the effective propagator. In the former case, this generates a structure which is

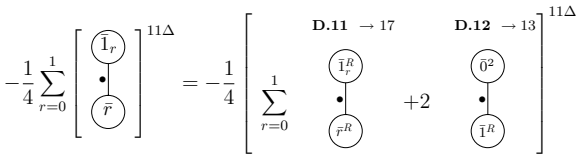

Figure 12. Isolation of the two-point, tree level vertices of diagram D.9.

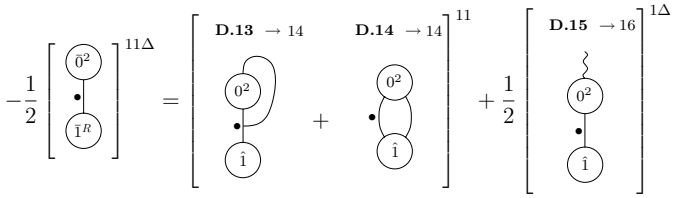

Figure 13. Decorating the two-point, tree level vertex of diagram D.12.

manifestly $\mathcal{O}(p^2)$, allowing us to Taylor expand at least some of the diagram's other structures in p. In the latter case, we can apply the effective propagator relation.

To facilitate the separation of the two-point, tree level vertices, we define the reduced, n-loop vertex thus:

$$v_n^R = \begin{cases} v_n & n > 0 \\ v_0 - v_{0RS}^{XX}(k) & n = 0, \end{cases}$$

where we have suppressed all arguments of the generic vertex, v_n, and its reduction. By definition, the reduced vertex does not contain a two-point, tree level component. A superscript number in a vertex argument denotes the total number of fields which must decorate the given vertex, e.g. 0^2 is the argument of a two-point, tree level vertex. Using this notation, we isolate the two-point, tree level vertices of diagram D.9 in figure 12.

Diagram D.12 simplifies. First, we note that $\bar{1}^R = \bar{1}$, by definition. Secondly, we note that

$$a_0\big[\bar{S}_n, \bar{S}_0^2\big] \equiv a_0\big[S_n, S_0^2\big] - a_0\big[S_n, \hat{S}_0^2\big] - a_0\big[\hat{S}_n, S_0^2\big] = -a_0\big[\hat{S}_n, S_0^2\big], \tag{22}$$

where the last step follows from the equality of the Wilsonian effective action and seed action two-point, tree level vertices. Performing this simplification, we decorate the two-point, tree level vertex, to give the diagrams of figure 13.

The relative factor of two in diagrams D.13 and D.14 comes from having been able to attach the effective propagator either way round. Explicit decoration with an external A^1 is denoted by a wiggly line, as exemplified in diagram D.15. Were we to decorate this diagram with the remaining external field, we would pick up a factor of 2, since the external fields would appear on different structures.

Diagrams D.13 and D.14 can be processed using the effective propagator relation (17), to give the terms of figure 14.

The structure of the calculation now begins to reveal itself, as we find two cancellations, which completely remove all seed action contributions generated by the action of a_1 in figure 8.

Cancellation 1. *Diagram D.16 exactly cancels the seed action contribution to diagram D.2.*

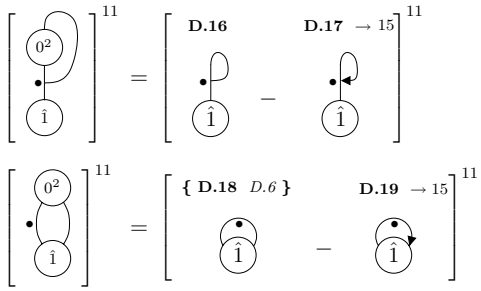

Figure 14. Processing diagrams D.13 and D.14 with the effective propagator relation.

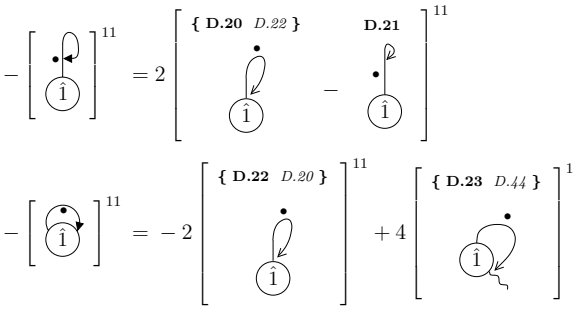

Figure 15. Result of processing the gauge remainders of diagrams D.17 and D.19.

Cancellation 2. *Diagram D.18 exactly cancels diagram D.6.*

The benefits of the refinements to the diagrammatic procedure are now becoming clear: had we explicitly decorated, e.g. diagrams D.6 and D.18 with the external fields, then the single cancellation 2 would be replaced by three separate cancellations; compared to the methodology of [6], we have succeeded in cancelling these terms in parallel. As the diagrammatic procedure is iterated, generating diagrams with increasing numbers of vertices, the number of terms cancelled in parallel grows rapidly, as we will see.

The gauge remainders of diagrams D.17 and D.19 can be processed using the techniques of section 3.2, to yield the terms of figure 15. The notation has been adapted since the active field, being an internal field, sits not only on the vertex struck by the gauge remainder but also at the end of a kernel. This kernel attaches to $>$ and so, rather than using the half-arrow notation of section 3.2, we use the $>$ to naturally indicate the momentum flow.

Following section 3.4, we have used charge conjugation to collect terms, i.e. the push forward and pull back onto a given field have been combined. In diagram D.23, an additional factor of two arises because the gauge remainder can strike either of the external fields. Note that decoration with the remaining external field now just yields a factor of unity.

Cancellation 3. *Diagram D.22 exactly cancels diagram D.20.*

Our next task is to examine diagram D.15. Since we are working at $\mathcal{O}(p^2)$, and this diagram possesses a structure which is manifestly $\mathcal{O}(p^2)$, we expect to be able to directly Taylor expand the rest of the diagram to zeroth order in p. In the case of this particular diagram, this

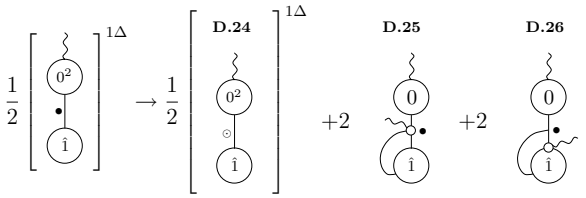

Figure 16. Processing diagram D.15 using the techniques of section 3.3.

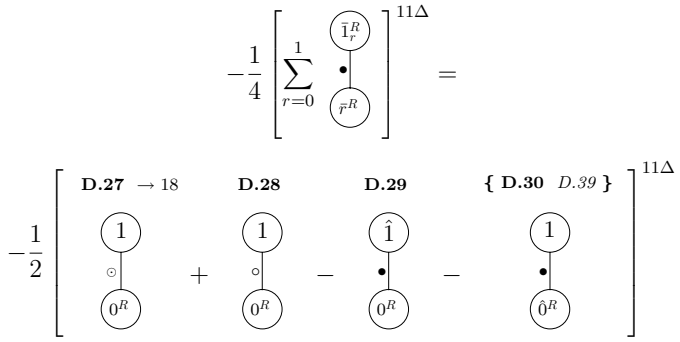

Figure 17. A re-expression of diagram D.11.

naïve expectation is correct. More generally, individual diagrams with an $\mathcal{O}(p^2)$ stub may not be Taylor expandable in p; rather, only sums of diagrams can be Taylor expanded [5, 7], since this procedure can generate IR divergences in individual terms. For reasons that will become apparent, it is actually only worth performing a Taylor expansion in the case that the kernel is decorated (before the Taylor expansion is performed). Diagram D.15 is processed in figure 16.

There are two things to note. First, in diagrams D.25 and D.26, the top end of the kernel carries zero momentum (at $\mathcal{O}(p^2)$) and the bottom end carries the same momentum as the decorative field (not to be confused with the derivative symbol). We have thus combined terms as discussed under equation (10). Secondly, we have not included any diagrams in which the kernel is decorated by the external field and either one loop or no loops. As we know from section 3.4, all such diagrams vanish by charge conjugation invariance, upon recognizing that the internal field attached to the two-point, tree level vertex must be an A^1.

The strategy is now very simple: we iterate the whole procedure. For each of diagrams D.3, D.10 and D.11, we can separate off a manipulable component, which we then convert into a Λ-derivative term. Amongst the terms generated will be a dumbbell structure, possessing at least one two-point, tree level vertex. Decorating the two-point, tree level vertices, we can either use the effective propagator relation or we can perform manipulations at $\mathcal{O}(p^2)$. There is one subtlety concerning the terms generated when we perform the conversion into Λ-derivative terms, which can be illustrated by considering diagram D.11; we isolate the manipulable component in figure 17. In figure 18, we convert diagram D.27 into a Λ-derivative term plus corrections.

To proceed, we process both diagrams D.34 and D.35, using the weak coupling flow equations. This is straightforward in the former case and we will not do it explicitly. In the

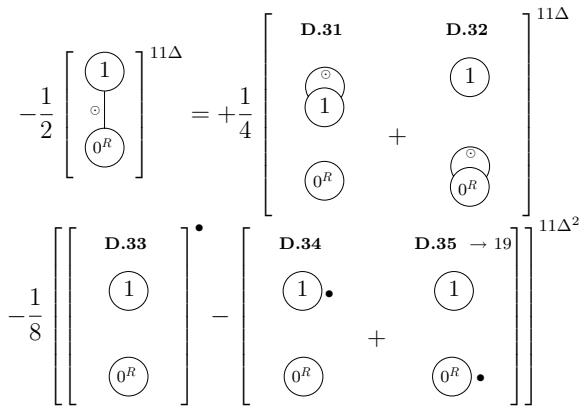

Figure 18. Converting diagram D.27 into a Λ-derivative term plus corrections.

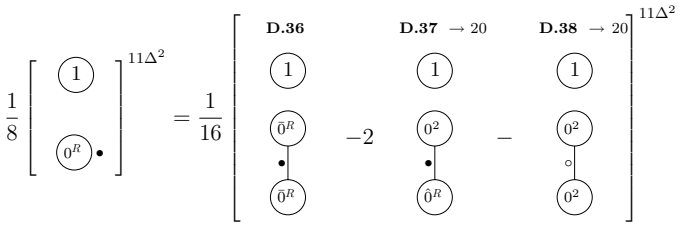

Figure 19. Processing diagrams D.34 and D.35 using the tree level flow equations.

latter case, we must understand how to compute the flow of a reduced, (tree level) vertex. The point is that a reduced vertex lacks a two-point, tree level component, and so the flow of a reduced vertex must lack the flow of a two-point, tree level vertex. From section 3.5.2, we know that the flow of a two-point, tree level vertex generates two two-point, tree level vertices, joined together by an undecorated kernel. Hence, the flow of a reduced tree level vertex must generate a dumbbell structure for which either at least one vertex is reduced or for which the kernel is decorated. Simplifying the barred notation, where possible, according to (22), we obtain the diagrams of figure 19.

The next step is the decoration of the two-point, tree level vertices of diagrams D.37 and D.38. Not all of the resultant terms are drawn, but rather the selection shown in figure 20.

As expected, we find cancellations.

Cancellation 4. *Diagram D.39 exactly cancels diagram D.30.*

Cancellation 5. *Diagram D.41 exactly cancels diagram D.5.*

Had we explicitly decorated diagrams D.39 and D.30 with the external fields and effective propagator, then the single cancellation 4 would be replaced with 24 separate cancellations[6]!

[6] For this particular diagram, this number could be considerably reduced by working at $\mathcal{O}(p^2)$ and noting that neither one-point, tree level vertices nor one point, Wilsonian effective action vertices (of any loop order) exist. However, the effects of such considerations must be worked out on a diagram-by-diagram level. Furthermore, in the current

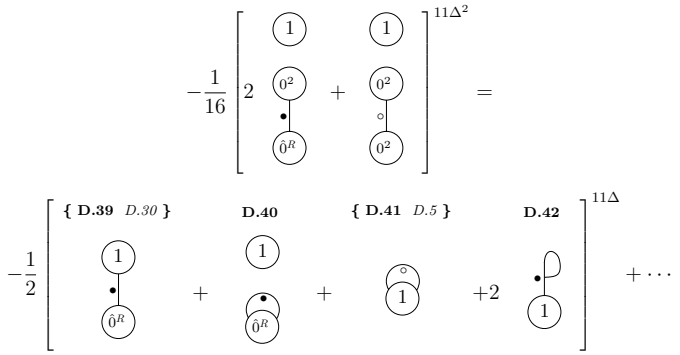

Figure 20. Partial decoration of diagrams D.37 and D.38.

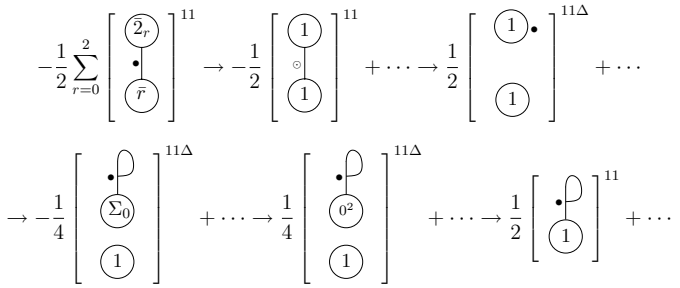

Figure 21. A sequence of terms spawned by diagram D.3.

Given that the two-loop diagrammatics can ultimately generate diagrams possessing four vertices and five internal lines, it is clear what a huge simplification the new techniques offer over the old methodology.

Notice, though, that diagram D.42 does not exactly cancel the Wilsonian effective action component of diagram D.2: to complete the cancellation, we must process diagram D.3. Specifically, we should focus on the $r = 1$ term. A sequence of terms derived from this diagram is shown in figure 21, culminating in the diagram we require to complete the cancellation of the Wilsonian effective action component of diagram D.2.

Iterating the diagrammatic procedure until exhaustion, we find that, up to gauge remainder terms and terms that require manipulation at $\mathcal{O}(p^2)$, the calculation reduces to α, β and Λ-derivative terms. The only cancellations involved in this procedure that we have not seen are those which remove terms such as D.31, D.32 and D.40.

The way in which these terms are cancelled is simple. Notice that bottom two structures of the latter two diagrams combine to form a contribution to Σ_0; were we to perform the complete diagrammatics, we would find the missing components. The resulting diagram would then cancel against a term spawned from the manipulation of diagram D.3; indeed, this term is included in the ellipsis after the fourth term of figure 21.

approach, there is no need to apply such constraints at this stage of the diagrammatics, since the cancellations are blind to such details, anyway. Ultimately, the constraint that Wilsonian effective action one-point vertices do not exist need only be used to simplify the final set of Λ-derivative terms.

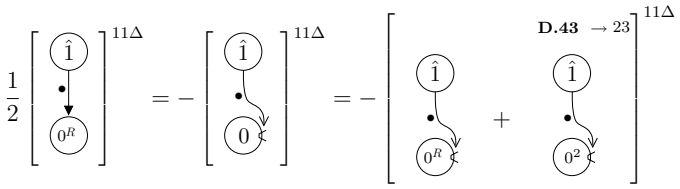

Figure 22. Example of a gauge remainder generated from iterating the diagrammatic procedure.

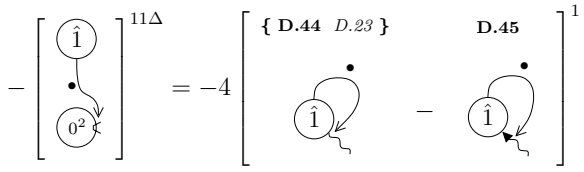

Figure 23. A selection of terms arising from the partial decoration of diagram D.43.

We conclude our illustration of the diagrammatic techniques with some further examples of gauge remainders and manipulations at $\mathcal{O}(p^2)$. First, consider the diagrams of figure 22.

On the left-hand side, we have a gauge remainder term. On the right-hand side, we have allowed the gauge remainder to act but have not specified which field it strikes, by employing the socket notation of [5]. This socket can be filled by any of the decorations. We have combined the push forward and pull back onto the socket, using charge conjugation invariance, choosing to represent the pair as a pull back (hence the factor of -2, compared to the parent).

Notice that a gauge remainder striking a reduced vertex generates a full vertex. This is trivial to see: since two-point, tree level vertices are killed by gauge remainders, we can promote a reduced vertex struck by a gauge remainder to a full vertex. Given that the action of the gauge remainder generates a full two-point, tree level vertex, our strategy is as before: we isolate any two-point, tree level contributions and partially decorate them. Amongst the terms generated by this latter procedure are those of figure 23.

Cancellation 6. *Diagram D.44 exactly cancels diagram D.23.*

Diagram D.45 is an example of a nested gauge remainder. The action of the nested gauge remainder is exactly the same as for any other gauge remainder. However, we recall from section 3.4 that we cannot generally use charge conjugation invariance to collect together diagrams in which the nested gauge remainder has acted.

The next example will demonstrate how diagrams involving processed gauge remainders can be converted into Λ-derivative terms. Consider the diagrams in figure 24. Notice that the first term is closely related to diagram D.21.

Diagram D.47 possesses a structure we have not yet encountered: the two-point, tree level vertex is attached exclusively to internal fields but cannot be removed by the effective propagator relation. Its top socket attaches to a differentiated effective propagator, whereas the attachment of an effective propagator to its bottom socket is interrupted by a processed gauge remainder. However, we can make progress by utilizing diagrammatic identities (7*a*),

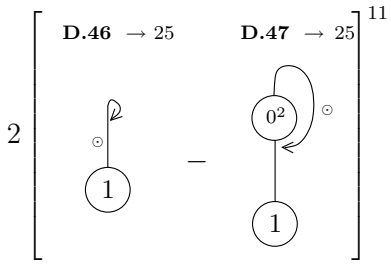

Figure 24. Two diagrams possessing processed gauge remainders which can be converted into a Λ-derivative term.

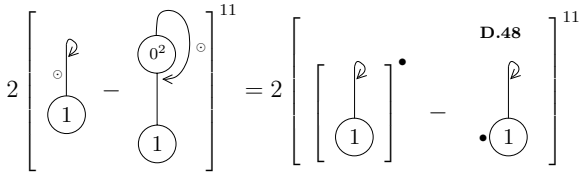

Figure 25. Conversion of diagrams D.46 and D.47 into a Λ-derivative term.

(17)–(20) and the tree level flow equation. We have

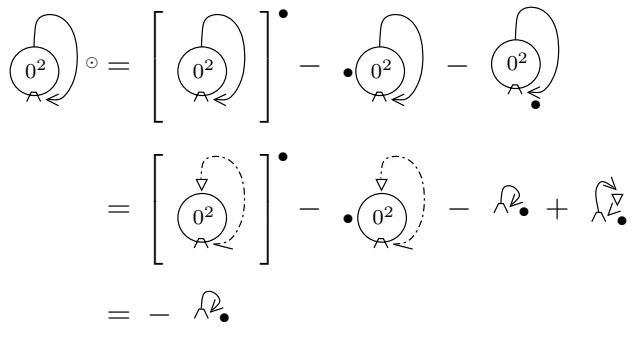

(23)

To go from the first line to the second, we have employed diagrammatic identity (20) and the effective propagator relation. On the second line, the first term vanishes courtesy of diagrammatic identity (18); similarly, the second term, if we employ (7*a*). The final term on the second line vanishes on account of diagrammatic identities (19) and (7*a*):

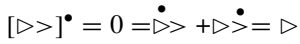

It is thus apparent that we can re-write diagrams D.46 and D.47, as shown in figure 25.

Notice that, amongst the terms generated by processing diagram D.48, is a term which will cancel diagram D.21.

By processing all the gauge remainders, we can reduce the calculation to a set of α, β and Λ-derivative terms, up to those diagrams which require manipulation at $\mathcal{O}(p^2)$ and a set of diagrams which do not manifestly cancel. It is easy to find an example of terms of the

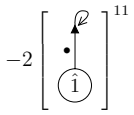

Figure 26. A gauge remainder term which cannot be processed.

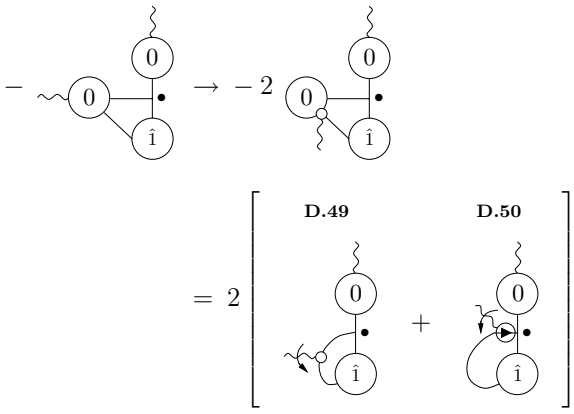

Figure 27. Example of a diagram which can be manipulated at $\mathcal{O}(p^2)$.

latter type. When diagram D.21 is cancelled, we know that a gauge remainder term will be left behind, as shown in figure 26.

The full gauge remainder is trapped and cannot be processed. The resolution to this problem is trivial, in this case: by charge conjugation invariance, the (necessarily bosonic) kernel has support only in the C^1 and C^2-sectors; but these are precisely the sectors where gauge remainders are null.  is a (trivial) example of a secondary diagrammatic identity. As we iterate the diagrammatic procedure, we find more complicated examples. The first non-trivial case is [5]

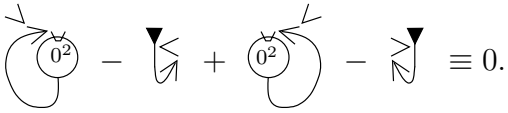

This is one of a family of secondary diagrammatic identities required for the computation of β_2, which are given in [5, 6]. The arbitrary loop generalization will be presented in [36].

Finally, we will deal with an example involving manipulations at $\mathcal{O}(p^2)$, which in turn generate gauge remainders. First, consider the fully decorated diagram on the left-hand side of figure 27, which we manipulate at $\mathcal{O}(p^2)$. To get to the second line, we have recognized that

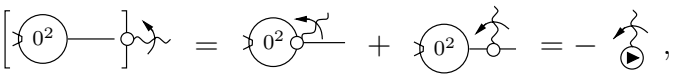

as a consequence of the effective propagator relation (where, strictly, this is only true when the structures involved are part of some complete diagram cf (17)).

Diagrams D.25, D.26 and D.49 combine into a total derivative with respect to the momentum flowing around the loop. However, the preregularization necessary to properly

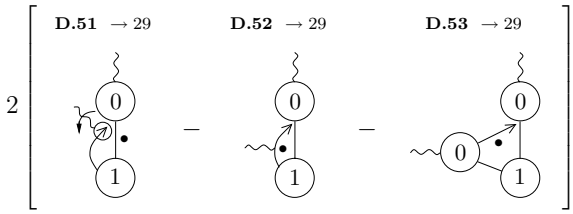

Figure 28. A selection of three terms possessing an $\mathcal{O}(p^2)$ stub.

define the $SU(N|N)$ regularization scheme [30] ensures that such terms vanish. Clearly, this happens automatically if we employ dimensional regularization as a preregularizer. However, as we will explore more fully in [36], it seems likely that we can instead adopt a diagrammatic prescription whereby sets of diagrams such as D.25, D.26 and D.49 can be discarded, purely from the standpoint that they can be diagrammatically cast as a total momentum derivative. This prescription would make sense in D strictly equal to 4.

With diagram D.50, it looks as though we might be stuck, since the gauge remainder is differentiated with respect to momentum. However, trivially redrawing

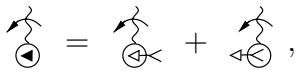

it is clear that progress can be made. In the case that the derivative hits the $>$, the $\triangleright$ strikes the kernel and can be processed as usual. In the case that the derivative hits $\triangleright$, we then use diagrammatic identity (20) to yield a $\triangleright$ striking the one-loop, seed action vertex. We will examine the former case but, rather than dealing directly with diagram D.50, will deal with the partner diagram (which we will not explicitly generate), coming with opposite sign, in which the one-loop vertex is a Wilsonian effective action vertex, rather than a seed action vertex. We focus on the term in which the gauge remainder pulls back along the kernel. Together with this diagram, we consider two diagrams which can be manipulated at $\mathcal{O}(p^2)$, as shown in figure 28.

Diagrammatically Taylor expanding the final two terms, we can cast the three diagrams of figure 28 as a Λ-derivative term. This is most easily seen by noting that

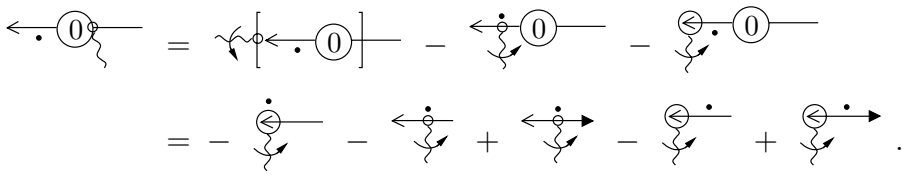

The first diagram on the second line follows in exactly the same way as (23). The other diagrams on the second line are simply obtained by using the effective propagator relation. Applying the above relation to diagram D.53 generates five diagrams. The third and fifth die, since they involve a gauge remainder striking a Wilsonian effective action, two-point vertex. The second diagram cancels diagram D.52, after the latter diagram is manipulated at $\mathcal{O}(p^2)$. The remaining two diagrams combine with diagram D.51 to form a Λ-derivative term, as shown in figure 29. Note that, at $\mathcal{O}(p^2)$, we can take the $\Lambda\partial_\Lambda|_\alpha$ to strike the entire diagram, i.e. including the two-point, tree level vertex decorated by the external field; this follows because the $\mathcal{O}(p^2)$ stub is independent of Λ.

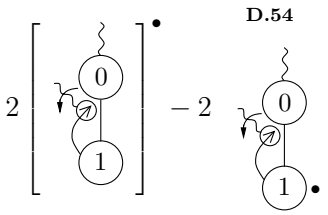

Figure 29. Rewriting diagrams D.51–D.53 as a Λ-derivative term.

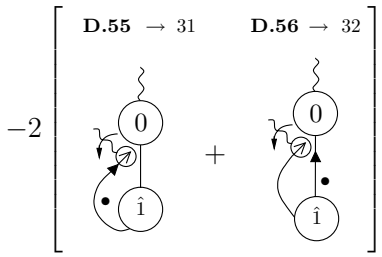

Figure 30. Trapped gauge remainders generated by processing diagram D.54.

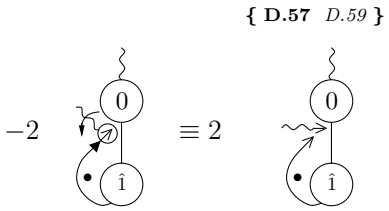

Figure 31. Exact redrawing of diagram D.55.

The final points can be made by considering manipulating diagram D.54. We know that the flow of the one-point vertex will generate, amongst other terms, the usual dumbbell structure possessing a two-point, tree level vertex. Applying the effective propagator relation, the Kronecker-δ terms will cancel diagrams generated elsewhere, leaving behind the trapped gauge remainders shown in figure 30.

Both diagrams D.55 and D.56 can be redrawn. In the former case, we first note from diagrammatic identity (19) that we can move the momentum derivative from $>$ to $\triangleright$, at the expense of a minus sign. Now, since it is true that, in all sectors for which the gauge remainder is not null,

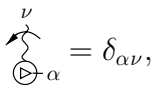

we can redraw diagram D.55 as shown in figure 31.

Diagram D.56 is redrawn, as shown in figure 32.

In the second diagram, if the left-most gauge remainder pushes forward, onto the internal field, we regenerate the parent. If this gauge remainder pulls back onto the internal field, the

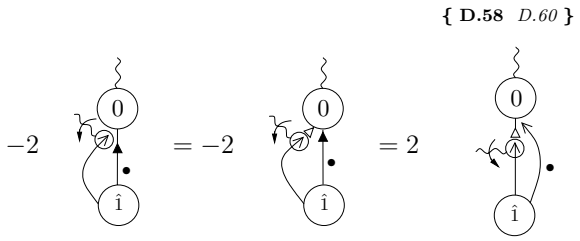

Figure 32. Exact redrawing of diagram D.56.

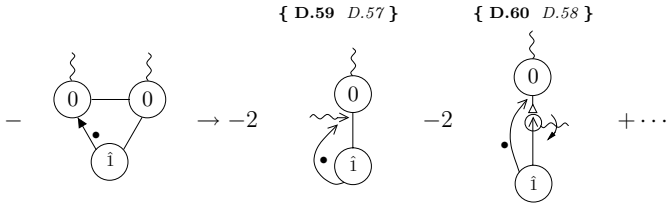

Figure 33. Generation of the diagrams to cancel D.55 and D.56.

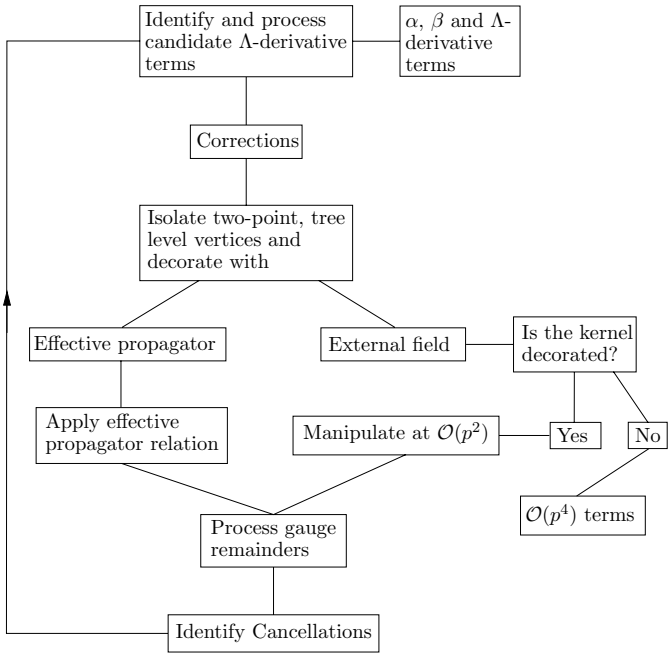

Figure 34. The diagrammatic procedure.

supertrace structure of the diagram is uniquely determined to be $\operatorname{str} A^1_\mu \operatorname{str} A^1_\nu = 0$. If either gauge remainder strikes the external field, we are left with a two-point, tree level vertex struck by a gauge remainder, which vanishes by diagrammatic identity (18). To go from the second diagram to the third, we allow the right-most gauge remainder to act; the only surviving contribution is the pull back onto the internal field, giving diagram D.58.

Redrawing diagrams D.55 and D.56 in this manner now allows us to understand how they are cancelled. In figure 33, we show the parent diagram, amongst the daughter diagrams of which, are the terms which yield the cancellations we are looking for.

Cancellation 7. *Diagram D.59 exactly cancels diagram D.57.*

Cancellation 8. *Diagram D.60 exactly cancels diagram D.58 upon recalling that charge conjugation invariance allows us to reflect a diagram, picking up a sign for each performed gauge remainder and each momentum derivative.*

These cancellations could have been performed directly against diagrams D.55 and D.56 by noting that the redrawing of figures 31 and 32 can be thought of as applications of (new) secondary diagrammatic identities. Cancellations 7 and 8 complete the illustration of the β_2 diagrammatics; the diagrammatic procedure is summarized in the flow chart of figure 34.

Iterating the entire procedure until exhaustion, we can reduce the calculation to a set of α, β and Λ-derivative terms and a set of '$\mathcal{O}(p^4)$ terms'. Diagram D.24 is an example of a term of the latter type; it can be easily demonstrated, using the Ward identities, that the sum of these terms vanish at $\mathcal{O}(p^2)$ [5, 6]. The Λ-derivative and β-terms can be simplified by utilizing the diagrammatic expression for β_1 [5, 7], to yield an expression for β_2 in terms of just α and Λ-derivative terms. As mentioned already, the α-terms vanish in the limit that $\alpha \to 0$. It is beyond the scope of this paper to describe the extraction of the numerical coefficient from the final set of terms; these techniques are fully described in [5, 7] (see also [34] for an example of their application in a simplified context).

Acknowledgment

I acknowledge financial support from PPARC.

References

[1] Morris T R 2000 *Nucl. Phys.* B **573** 97 (*Preprint* hep-th/9910058)
[2] Morris T R 2000 *J. High Energy Phys.* JHEP12(2000)012 (*Preprint* hep-th/0006064)
[3] Arnone S, Gatti A and Morris T R 2003 *Phys. Rev.* D **67** 085003 (*Preprint* hep-th/0209162)
[4] Rosten O J, Morris T R and Arnone S 2004 The gauge invariant ERG *Proc. Quarks 2004 (Pushkinskie Gory Russia 24–30 May 2004)* http://quarks.inr.ac.ru *Preprint* hep-th/0409042
[5] Rosten O J 2005 The manifestly gauge invariant exact renormalisation group *PhD Thesis* University of Southampton (*Preprint* hep-th/ 0506162)
[6] Arnone S, Morris T R and Rosten O J 2005 *Preprint* hep-th/0507154
[7] Morris T R and Rosten O J 2006 *Phys. Rev.* D **73** 065003 (*Preprint* hep-th/0508026)
[8] Gribov V N 1978 *Nucl. Phys.* B **139** 1
[9] Fisher M E 1998 *Rev. Mod. Phys.* **70** 653
[10] Morris T R 1998 *Prog. Theor. Phys. Suppl.* **131** 395 (*Preprint* hep-th/9802039)
[11] Litim D F and Pawlowski J M 1999 *Preprint* hep-th/9901063
[12] Aoki K 2000 *Int. J. Mod. Phys.* B **14** 1249
[13] Berges J, Tetradis N and Wetterich C 2002 *Phys. Rep.* **363** 223 (*Preprint* hep-ph 0005122)
[14] Bagnuls C and Bervillier C 2001 *Phys. Rep.* **348** 91 (*Preprint* hep-th/0002034)
[15] Polonyi J 2003 *Cent. Eur. J. Phys.* **1** 1 (*Preprint* hep-th/0110026)
[16] Salmhofer M and Honerkamp C 2001 *Prog. Theor. Phys.* **105** 1
[17] Delamotte B, Mouhanna D and Tissier M 2004 *Phys. Rev.* B **69** 134413 (*Preprint* cond-mat 0309101)
[18] Wilson K and Kogut J 1974 *Phys. Rep.* C **12** 75
[19] Wegner F J and Houghton A 1973 *Phys. Rev.* A **8** 401
[20] Polchinski J 1984 *Nucl. Phys.* B **231** 269
[21] Pawlowski J M 2005 *Preprint* hep-th/0512261
[22] Reuter M and Wetterich C 1994 *Nucl. Phys.* B **417** 181

[23] Freire F, Litim D F and Pawlowski J M 2000 *Phys. Lett.* B **495** 256 (*Preprint* hep-th/0009110)
[24] Litim D F and Pawlowski J M 2002 *J. High Energy Phys.* JHEP09(2002)049 (*Preprint* hep-th/0203005)
[25] Litim D F and Pawlowski J M 2002 *Phys. Lett.* B **546** 279 (*Preprint* hep-th/0208216)
[26] Bonini M, D'Attanasio M and Marchesini G 1994 *Nucl. Phys.* B **421** 429 (*Preprint* hep-th/9312114)
[27] Bonini M, D'Attanasio M and Marchesini G 1995 *Nucl. Phys.* B **437** 163 (*Preprint* hep-th/9410138)
[28] Ellwanger U 1994 *Phys. Lett.* B **335** 364 (*Preprint* hep-th/9402077)
[29] D'Attanasio M and Morris T R 1996 *Phys. Lett.* B **378** 213 (*Preprint* hep-th/9602156)
[30] Arnone S, Kubyshin Y A, Morris T R and Tighe J F 2002 *Int. J. Mod. Phys.* A **17** 2283 (*Preprint* hep-th/0106258)
[31] Latorre J I and Morris T R 2000 *J. High Energy Phys.* JHEP11(2000)004 (*Preprint* hep-th/0008123)
Latorre J I and Morris T R 2001 *Int. J. Mod. Phys.* A **16** 2071 (*Preprint* hep-th/0102037)
[32] Arnone S, Gatti A and Morris T R 2002 *J. High Energy Phys.* JHEP05(2002)059 (*Preprint* hep-th/0201237)
[33] Arnone S, Gatti A, Morris T R and Rosten O J 2004 *Phys. Rev.* D **69** 065009 (*Preprint* hep-th/0309242)
[34] Arnone S, Morris T R and Rosten O J 2005 *J. High Energy Phys.* JHEP10(2005)115 (*Preprint* hep-th/0505169)
[35] Rosten O J 2005 *Preprint* hep-th/0511107
[36] Rosten O J 2006 *Preprint* hep-th/0602229
[37] Bars I 1984 *Introduction to Supersymmetry in Particle Nuclear Physics* ed O Castanõs *et al* (New York: Plenum) p 107
[38] Morris T R 1999 *The Exact Renormalization Group* ed A Kraznitz *et al* (Singapore: World Scientific) p 1 (*Preprint* hep-th/9810104)